Deck-tower interaction in the transverse seismic response of cable-stayed bridges and optimum configurations

A. Camara[1], E. Efthymiou[1]

(1) Department of Civil Engineering. City University London. Northampton Square, London EC1V 0HB, United Kingdom

Cite as: A. Camara, E. Efthymiou (2016). Deck-tower interaction in the transverse seismic response of cable-stayed bridges and optimum configurations. Engineering Structures, 124:494-506.

Abstract

Modern design solutions in cable-stayed bridges give a significant importance to the seismic response in the transverse direction. This work is focused on the dynamic interaction between the deck and the towers, exploring the key role of different vibration modes. An extensive parametric analysis is proposed to address the influence of the main span length, the tower geometry, the cable-system arrangement, the width and height of the deck and the soil conditions. It is demonstrated that the vibration modes that govern the seismic response of cable-stayed bridges in the transverse direction involve the interaction between the tower and the deck, but the order of these modes and the parts of the deck that are affected change with the main span length. It is also observed that the interaction between the deck and the towers during the earthquake is maximised if their isolated vibration frequencies are close to each other, leading to a significantly large seismic demand. Analytical expressions are proposed to obtain the critical frequencies of the towers for which these interactions arise, and recommendations are given to define the tower geometry in order to avoid such problematic scenarios.

Email addresses: Alfredo.camara@city.ac.uk (A. Camara[1]), Eleftheria.Efthymiou@city.ac.uk (E. Efthymiou[1])

Keywords:
Cable-stayed bridges; seismic response; high-order vibration modes; tower-deck interaction; tower shape; cable arrangement; deck width.

1. Introduction

Cable-stayed bridges represent optimum solutions for an ever expanding range of spans and usually constitute the backbones of infrastructure networks. Their design is governed by the response to dynamic actions such as wind or earthquakes due to their characteristic flexibility and low damping [1]. Furthermore, complex modal couplings arise from the interaction between the towers, the deck and the cable-system and depend upon their relative stiffness and mass, as well as the frequency content of the excitation [2, 3]. It is essential to have a clear understanding on these effects in order to ensure the adequate response of the structure under different loading scenarios.

The vibration of the cables can transfer energy between the deck and the towers during the earthquake [4] but, depending on the support conditions, the direct interaction between both members is potentially more significant. The connection of the deck to the abutments, intermediate piers and (especially) to the towers affects the response of the whole structure [5]. A considerable number of works address the influence of the deck-tower connection from the point of view of the static [6, 7] and the seismic response [8, 9, 10, 11, 12]. The current trend in the design of cable-stayed bridges in seismic areas is to release the deck from the towers as much as possible in order to reduce the seismic demand in the towers, which are key elements for the integrity of the structure [13]. However, the deck needs to be fixed to the towers in the transverse direction in order to control its deformability under wind actions (e.g. Rion-Antirion bridge, Greece). Recent studies on cable-stayed bridges with this type of connection have found that the deck-tower reaction significantly increases the transverse shear force and bending moment in the towers, making the transverse component of the earthquake more demanding than the longitudinal (along-deck) and vertical directions [14, 15]. Indeed, the damage in the tower of the Chi-Lu bridge tower during the Chi-Chi earthquake (Taiwan 1999) can be directly attributed to the transverse response, and it is arguably the most severe seismic damage ever reported in a cable-stayed bridge [16]. Unfortunately, studies focused on the transverse seismic response of cable-stayed bridges are scarce.

The magnitude of the transverse deck-tower reaction is determined by the interaction between several bridge components with very different dynamic properties, i.e. the deck, the towers and the cable-system. Different vibration modes involving the deformation of one or more of these three components play an essential role in the seismic response. Cable-stayed bridges below 400 m main span length present important modal couplings between the deck and the towers that affect the fundamental vibration modes [3]. However, in long-span bridges the first vibration mode involves exclussively the transverse flexure of the deck, with little or no interaction with the towers [17]. The large flexibility, important modal couplings and the typical broad frequency content of ground motions make the seismic response of cable-stayed bridges prone to strong high-order mode contributions (up to 25Hz frequency), as observed in [18]. Code-based seismic analyses typically include as many vibration modes as needed to activate a certain percentage of the mass of the bridge, usually 90%. As a result, the relative contribution of different modes is not clearly considered in the design, which is based on iterative techniques that rely upon the experience of the designer [7]. Different authors proposed design techniques to define the cable prestressing forces in order to meet several requirements [19, 20]. Few works include dynamic actions in the design procedure. Ferreira and Simoes [21] proposed a formulation to design a two-dimensional cable-stayed bridge with active control devices under longitudinal ground motion, without considering the influence of the tower shape. Calvi *et al.* [22] presented a conceptual design method that accounts for the seismic actions as well as the deck and tower configurations in the longitudinal and transverse directions, recommending further studies on the seismic response of the towers with transverse struts. Hayashikawa *et al.* [23] studied the seismic behaviour of steel towers in which the effect of the cable-system was simplified with equivalent springs and the interaction with the deck was ignored. However, the importance of this effect has been recently observed by [3, 14, 13].

To the best of the author's knowledge, there are no previous papers focused on the transverse seismic response of cable-stayed bridges accounting for the contribution of different vibration modes and the influence of the tower shape, among other structural features. This is the scope of the present work, which presents an extensive numerical analysis in a wide range of main span lengths, tower shapes, cable-arrangements, deck widths and distances between the deck and the foundation level. Altogether, a total of 1050 three-dimensional Finite Element (FE) models are studied. After presenting the proposed structures, the vibration modes of the individual towers and the complete bridges are studied. Two different analysis methods and modelling techniques are then compared. The Modal Response Spectrum Analysis (MRSA) represents the optimum balance between calculation speed and accuracy (for the purpose of the study), and it is adopted. As the main span length increases, it is observed that the transverse response is mainly dominated by higher-order modes that involve different parts of the deck. The tower geometry, deck width and height significantly influence the contribution of the governing modes, which allows for optimum designs aiming to reduce the seismic response. This work also demonstrates that the seismic response and the interaction between the deck and the tower in the transverse direction is maximised when their frequencies (calculated separately) are close to each other, proposing simple analytical expressions to predict these problematic scenarios.

2. Description of the proposed bridges

The bridges considered in this work have a conventional symmetric configuration with a composite (steel-concrete) girder and two concrete towers. Figure 1 presents the different tower shapes proposed, the elevation and plan views, and the keywords employed to refer to the results in the following sections. The cross-sections of the tower, girder and cable-system are defined in terms of the main span length (L_P), which also configures the side spans (L_S) and the tower height above the deck (H). A complete description of the bridge sections and dimensions is available in [3]. Two different semi-harp cable arrangements have been defined: two Lateral Cable Planes (LCP) or a single Central Cable Plane (CCP). The deck has a composite (steel-concrete) cross-section that is constant along the length of the bridge and depends on the cable-arrangement: (1) LCP models present an open deck cross-section with two edge I-shape steel girders and a 25 cm thick concrete slab spanning transversely, (2) the deck in CCP bridges has a U-shape steel girder that forms with the top slab a closed-box section and provides with additional torsional resistance. The support conditions of the deck at the abutments and the towers are depicted in Figure 1. The intermediate piers only constrain the vertical movement of the deck. The deck is rigidly connected to the towers in the transverse direction (Y), whilst it is released in the longitudinal (X) and vertical (Z) directions.

The parametric study is based upon the main span length (L_P), which

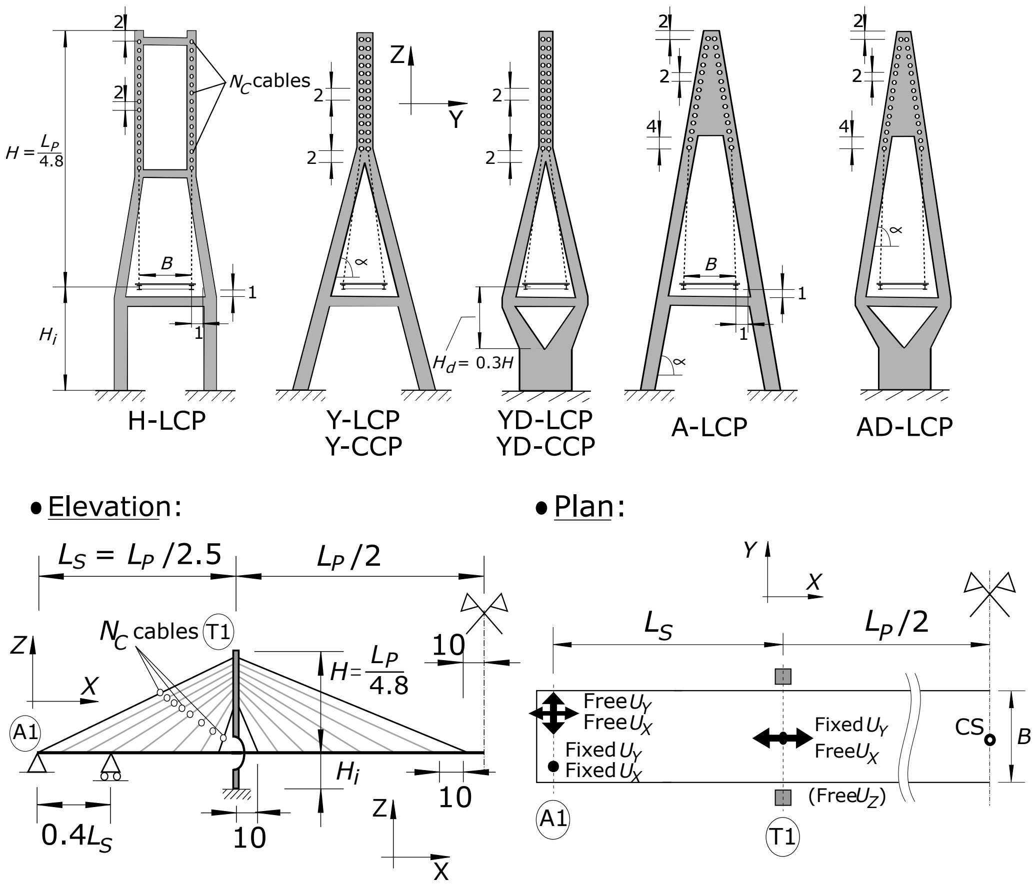

Figure 1: Parametrisation of the studied bridges, including the tower shape and the corresponding keywords. Units in meters.

completely defines all the elements of the bridge, with the exception of the width of the deck (B) and the distance between the foundation of the tower and the deck level (H_i, Figure 1). The main span is modified from 200 to 800 m, each 10 m, considering four different deck widths: $B = 20, 25, 30, 35$ m and a conventional value for the deck level ($H_i = H/2$). In addition, two more values of H_i are considered for the whole span range: $H_i = H/1.5$ and $H_i = H/2.5$, setting the deck width to $B = 25$ m. Altogether, 1050 bridge models are implemented in a general-purpose finite element analysis package [24]. The elastic properties in the studied bridges are defined from the relevant Eurocodes [25, 26]. No material nonlinearities have been considered.

A number of initial studies were conducted to ensure the accuracy and suitability of the modelling assumptions:

- The effect of the foundations at the towers in the H-LCP bridges was initially represented by means of springs, selecting their flexibility based on the dimensions of the foundation and the soil properties (both rock and soft soil conditions were considered). It was observed that the vibration modes below 3 Hz, which govern the transverse deck-tower reaction as discussed later, do not involve the movement of the bridge supports. Consequently, the supports of the towers, piers and abutments are completely fixed in this work in order to simplify the parametrisation of the model.

- The influence of the cable-structure interaction was explored in cable-stayed bridges with different main spans and central cable layouts (Y-CCP). It was observed that by including multiple elements per cable (MECS) the transverse deck-tower reaction is decreased by 0, 30 and 25% in bridges with 200, 400 and 600 m main span, respectively, in comparison with the homologue models with one element per cable (OECS), in agreement with [27]. The authors propose OECS for this study in order to facilitate the parametrisation and allow for the analysis of a large number of models. OECS is considered a valid approach in this study because the scope is not to achieve the best accuracy in the deck-tower reaction, but to explore the interaction between the deck and the towers in a large number of models. This interaction is not deemed to be affected by the local vibration of the cables due to their reduced weight.

3. Modal analysis

The modal analysis of the tower models (in which the deck and the cable-system are removed) is presented in Figure 2. The fundamental vibration modes are strongly influenced by the connections between the lateral legs.

The towers with inclined lateral legs connected exclusively above the deck (i.e. the inverted 'Y'- and 'A'-shaped geometries in Figure 1) present vibration frequencies (ω) that are up to 70% larger than in the rest of the towers. This is because the transverse movement of the connection point above the deck is constrained in the transverse direction due to the inclination of the legs, which is influenced in turn by the ratio between the width of the deck and the height of the tower (B/H). Consequently, inverted 'Y'- and 'A'-shaped towers will be referred to as 'stiff towers'. Figure 2 shows that the transverse displacement of the fundamental mode ($\boldsymbol{\phi}_1^Y$) at the connection between legs in the inverted 'Y'-shaped tower is almost null in the short-span bridge ($\boldsymbol{\phi}_1^Y \approx 0$ for Y-LCP with $L_P = 300$ m) because of this geometric constraint. By increasing the main span, the tower needs to be higher (its height above the deck is given by $H = L_P/4.8$) but the width of the deck remains constant since it mainly depends on the number of road lanes. Consequently, the transverse inclination of the legs (angle α in Figure 1) increases with the main span length and this effect is found to be stronger than the increment of the tower cross-sections. This results in larger modal displacements at the connection between the legs above the deck for longer spans ($\boldsymbol{\phi}_1^Y \approx 0.2$ for for Y-LCP with $L_P = 800$ m). An analogous effect is observed by reducing the width of the deck. Interestingly, the towers corresponding to bridges above 400 m span show zero modal displacement at the connection between the legs in the second-order transverse vibration mode ($\boldsymbol{\phi}_2^Y \approx 0$), and not in the fundamental one, which has an impact on the seismic response of medium-to-long span bridges as it will be discussed later.

The towers with 'lower diamond' configuration (D) present inclined legs that are connected above and below the deck. These are referred to as 'flexible towers' because the transverse restraint of the above-deck leg connection, that was apparent in the stiff towers, disappears in the towers with lower diamond due to the rotation at the connection below the deck ($\boldsymbol{\phi}_1^Y \approx 0.5$ for YD towers with $L_P = 300$ m in Figure 2). This effect will have a significant influence on the seismic response as well. Analogously, the rotation capacity of the lower diamond is influenced by the inclination of the lower legs, being proportional to the geometrical ratio B/H_d (where H_d is the distance between the deck and the top of the vertical pier, as it is represented in Figure 1). 'H'-shaped towers behave as Vierendeel beams in the transverse direction and are also classified as 'flexible towers'.

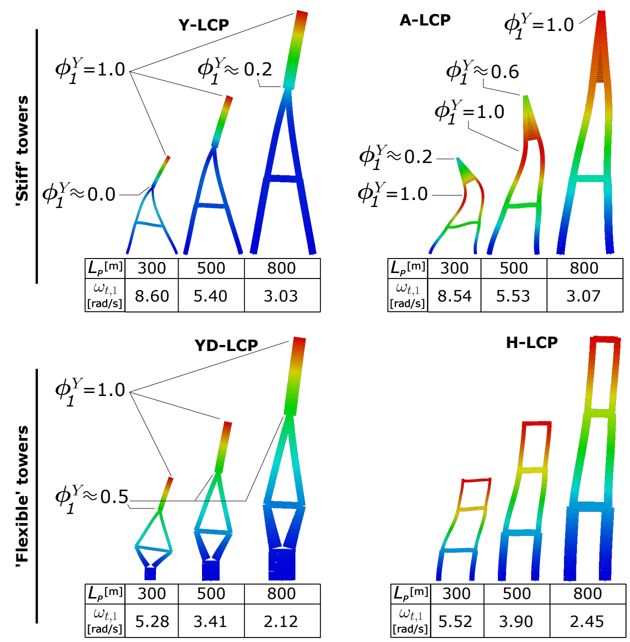

Figure 2: Fundamental mode shape and angular frequencies ($\omega_{t,1}$ in [rad/s]) of different tower models. The contour plot represents the normalised modal displacement in the transverse direction, ϕ_1^Y. LCP tower models. $H_i = H/2$, $B = 25$ m.

The complete bridge models (including the towers, the cable-system and the deck) have been also considered in the modal analysis. Cable-stayed bridges show a characteristic coupling between the transverse flexure and the torsion of the deck [2, 3]. An additional set of boundary conditions is included in order to allow only for transverse modes. To this end, the longitudinal displacement (u_X) of the towers and the vertical displacement (u_Z) of the deck are constrained. It is observed that the transverse vibration frequencies are not significantly influenced by these boundary conditions. Figure 3 presents the three governing transverse vibration modes in one of the proposed models (H-LCP): (i) mode M1 involves the first-order symmetric flexural response of the main span (L_P), (ii) mode S1 presents a first-order symmetric wave affecting the side spans (L_S), and (iii) mode M2 shows a second-order symmetric wave in the main span. The transverse vibration frequencies associated with these modes strongly decrease by increasing the main span length (L_P). Scaling L_P by a factor of 2.5 results in the transverse vibration frequencies that are 4.4 and 3.4 times smaller in the M1 and S1 modes, respectively. To explain this result, the transverse response of the deck can be described by means of a one-span beam with appropriate boundary conditions that represent the effect of the adjacent spans and the towers. In these circumstances the transverse vibration frequency is given by:

$$\omega_{d,n} = A\sqrt{\frac{EI_d}{m_d L^4}} \tag{1}$$

in which n is the order of the vibration mode; L is the length of the deck involved in the corresponding mode; E is the Young's modulus of the material in the deck; I_d and m_d are the transverse second moment of area and the mass per unit length of the deck, respectively; A is a constant that depends on the boundary conditions and n.

By increasing the main span length (L_P), I_d and m_d remain almost constant since the width of the deck does not depend on L_P and its depth is almost insensitive to this parameter (especially in LCP arrangements) [28]. Eq. (1) shows that a linear increment of L_P would reduce $\omega_{d,n}$ quadratically if we assume that A remains constant, i.e. that the restraint in the deck from the towers and adjacent spans does not change with L_P. However, the boundary conditions assumed in Eq. (1) are indeed affected by L_P. Figure 3 shows that the transverse flexure of the towers interacts with the deck only for specific span lengths and vibration modes. This effect is related to the relative flexibility between the deck and the towers.

In the vibration mode M1 the deck of the short-span bridge clearly interacts with the towers in the transverse direction ($L_P = 300$ m, cell A1 in Figure 3). This is because the vibration frequencies of the first-order vibration modes of the deck and the towers are similar, and their coupling will result in significantly large seismic effects (Section 7). The flexibility of the deck grows much faster with L_P than the flexibility of the towers. This is because the cross-sections of the tower legs need to be increased to resist the weight of the deck in longer bridges. Consequently, the deck and the towers do not interact in the fundamental mode (M1) of medium- and long-span cable-stayed bridges. In this span range, M1 presents no transverse deformation of the towers (i.e. no deck-tower interaction), and the vibration frequency is so low (below 1 rad/s for $L_P = 740$ m) that this mode hardly

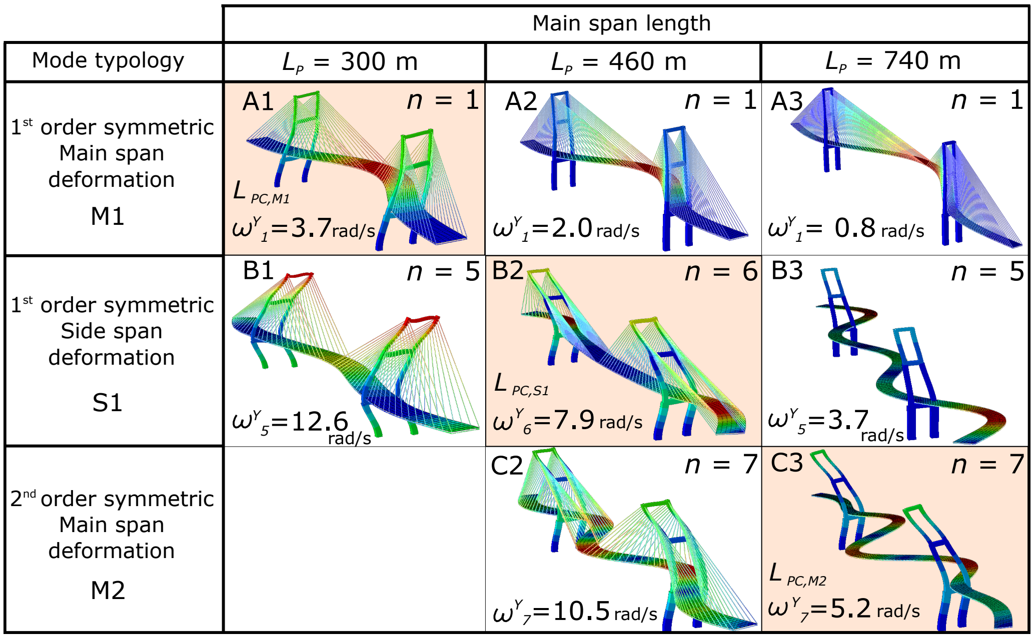

Figure 3: Mode shapes (ϕ^Y), mode order (n) and vibration frequencies (ω_n^Y) of the three dominant vibration modes for different main spans (L_P). The cable system is removed from B3 and C3 to improve clarity. M2 is not included for $L_P = 300$ m as it has not been clearly identified. H-LCP model, $B = 25$ m, $H_i = H/2$.

contributes to the seismic demand in terms of forces. Nonetheless, the mode S1 involves the deformation of a smaller part of the deck (i.e. the side spans, $L_S = L_P/2.5$). Therefore, its vibration frequency is higher than that in M1, and it is eventually coupled with the second-order vibration mode of the towers. The mode S1 shows interaction between the deck and the tower in bridges with medium span lengths (e.g. $L_P = 460$ m, cell B2) and it will result dominant in the transverse seismic response of structures in this span range. In very long-span cable-stayed bridges, typically above 700 m main span lengths, the transverse flexibility of the deck is so large that only the second-order flexure of the deck in the main span is able to interact with the second-order mode of the towers (mode M2, model with $L_P = 740$ m, cell C3 in Figure 3). The main span lengths for which these three modes involve the strongest deck-tower interaction are referred to as 'critical' (L_{PC}) and are highlighted in Figure 3.

4. Seismic analysis framework and proposed ground motions

The seismic action is defined by the EN1998-1 [29] horizontal acceleration spectra in rock (TA) and soft (TD) soil conditions, as shown in Figure 4. The Peak Ground Acceleration is 0.5 g and the damping ratio is 4% in order to consider the reduced damping of cable-stayed bridges. Type 1 spectrum is considered, with large surface-wave magnitude ($M_s > 5.5$). The same seismic action is applied at different supports of the bridge, thus ignoring spatial variability effects.

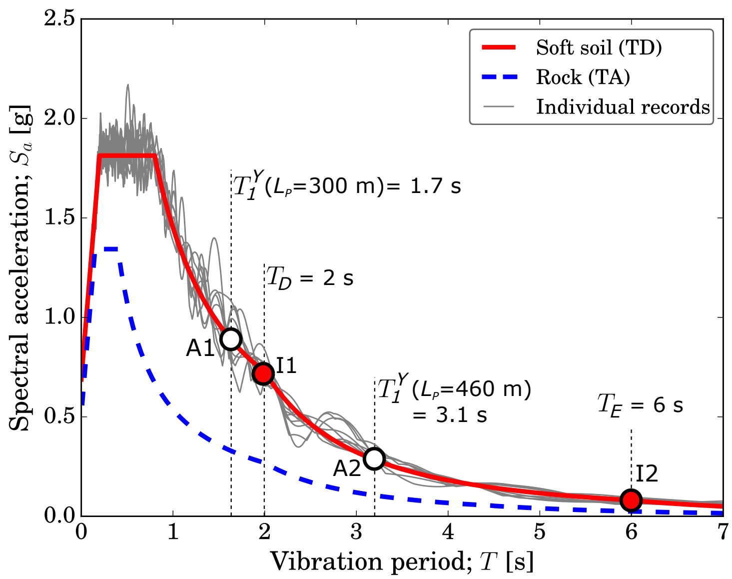

Figure 4: EN1998-1 acceleration spectra used in MRSA, and spectra of the artificial accelerograms in MRHA. $I1$ and $I2$ are related to the corner periods T_D and T_E in [29]. $A1$ and $A2$ refer to the fundamental periods in the H-LCP models ($B = 25$ m and $H_i = H/2$) for two different main spans.

It is important to select carefully the seismic analysis methodology due to the large number of models considered in this work. The Modal Response History Analysis (MRHA) is the most accurate method to study the linear elastic seismic response of cable-stayed bridges [30]. However, it requires the computation and post-processing of the time-history response of each model (1050 in total), repeating the analysis for a representative set of ground motions. Since this study is focused on the peak seismic response, Modal

Response Spectrum Analysis (MRSA) represents an ideal solution to reduce the computational time to a reasonable level. The results of MRSA are validated in this section by considering MRHA as the reference.

In order to study the transverse interaction between the deck and the towers, the transverse vibration modes need to be isolated from the rest (in particular the numerous modes with torsional coupling in the deck and negligible contribution). To this end, the longitudinal movement of the towers and the vertical movement of the deck are constrained (the resulting models are referred to as 'transverse models'). Figure 5 compares the peak deck-tower reaction (F^Y) resulting from MRSA applied to the transverse models and MRHA applied to the original models (i.e. without the added constraints to the tower and deck movements). A total of 12 synthetic accelerograms are applied synchronously at the bridge supports in the transverse direction in order to obtain the arithmetic mean (μ) and standard deviation (s) of the peak deck-tower connection in MRHA. Figure 4 shows how the records match the target acceleration spectra (for soft soil conditions) in the range of important vibration frequencies for the structure [0.15,35] Hz. The method to generate the signals has been discussed elsewhere [15, 30]. The total deck-tower reaction (F^Y_{total}) in MRHA includes the contribution of all the vibration modes below 35 Hz, whereas the corresponding result in MRSA combines the first ten transverse vibration modes (which are typically enough to exceed the upper frequency limit of 35 Hz). An initial study showed that the contribution of vibration modes beyond the 10-th transverse mode is negligible in MRSA.

Figure 5(a) includes the contribution of the governing vibration modes (M1, S1 or M2, considered separately) to the total deck-tower reaction in MRSA. In addition, this figure shows that the contribution of mode M1 increases rapidly with L_P and it becomes maximum at $L_{PC,M1} = 300$ m (Point A1). At this point the interaction between the tower and the main span of the deck is maximised. Figures 3 and 4 include the modal shape and the spectral acceleration associated with this case (Point A1), respectively. Points I1 and I2 in Figure 5(a) mark the spans beyond which the contribution of the fundamental mode to the transverse response decreases faster by increasing L_P. This is directly connected to the shape of the elastic spectrum included in Figure 4, which shows that I1 and I2 correspond to the corner periods proposed in EN1998-1 [29].

The total (mean) deck-tower reaction obtained in MRHA is in good agreement with the result obtained in MRSA, as it is shown in Fig. 5(b). The main spans for which the maximum deck-tower reaction occurs are also similar in both types of analysis. However, several vibration modes contribute to the MRHA results in Fig. 5(b). In order to investigate which is the dominant mode for $L_P = 300$ m (point A), the corresponding time-history signal of the deck-tower reaction obtained for one of the accelerograms using MRHA is expressed in the frequency-domain by means of the Fast Fourier Transform in Figure 6. The shapes of the most important modes arising from this study are also presented. Mode M1 is clearly responsible for the increment of F^Y_{total} in MRHA for the short-span bridge ($L_P = 300$ m). Analogously, the MRSA and MRHA results in Figures 5 and 6 identify the vibration modes S1 and M2 as dominant for bridges with medium ($L_{PC,S1} = 420 - 460$ m, point B) and long spans ($L_{PC,M2} = 720 - 740$ m, point C), respectively. The higher the order of the governing vibration mode, the stronger the coupling between the flexural and torsional responses in the deck in MRHA. This, in addition to the record-to-record variability in the acceleration spectra of the set of 12 ground motions (Figure 4), hinders the identification of the contribution of mode M2 to the mean MRHA results in Figure 5(b). Figure 6 also shows that the most important vibration frequencies for the deck-tower reaction fall between 0.2 and 1.8 Hz (1.3 and 11.3 rad/s), regardless of the main span length. This is also observed in Figure 3 for the frequencies of the vibration modes with maximum deck-tower interaction at the critical main spans. Beyond 3 Hz (18.8 rad/s) the vibration modes have no significant contribution to the deck-tower reaction.

The MRHA and MRSA results have been compared in cable-stayed bridges with other tower shapes in the entire span range. Figure 7 presents these results in CCP models (other cases are not included to improve the clarity in the figure). The difference between the results in both analyses is small (typically below 10%). MRSA including only transverse modes will be employed hereafter because the purpose of this study is not to calculate the magnitude of the deck-tower reaction with great accuracy. Instead, the goal is to explore how this reaction is affected by the interaction between the deck and the tower in different vibration modes, and this can be better studied with MRSA.

5. Multi-modal response

Figure 5(a) shows that the contribution of different vibration modes to the total deck-tower reaction is strongly influenced by the main span length.

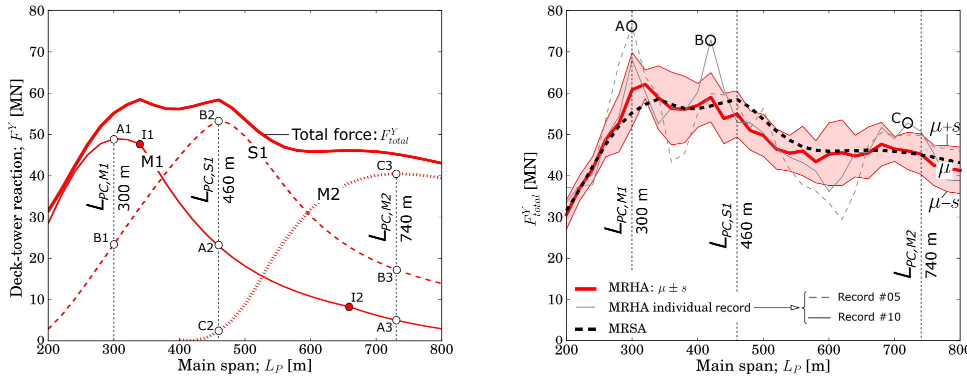

Figure 5: Peak deck-tower seismic reaction obtained with: (a) MRSA (only transverse modes included) with relevant mode-shapes presented in Figure 3; (b) MRHA, the governing mode-shapes for two particular records are included in Figure 6. H-LCP model, soil TD, $H_i = H/2$, $B = 25$ m.

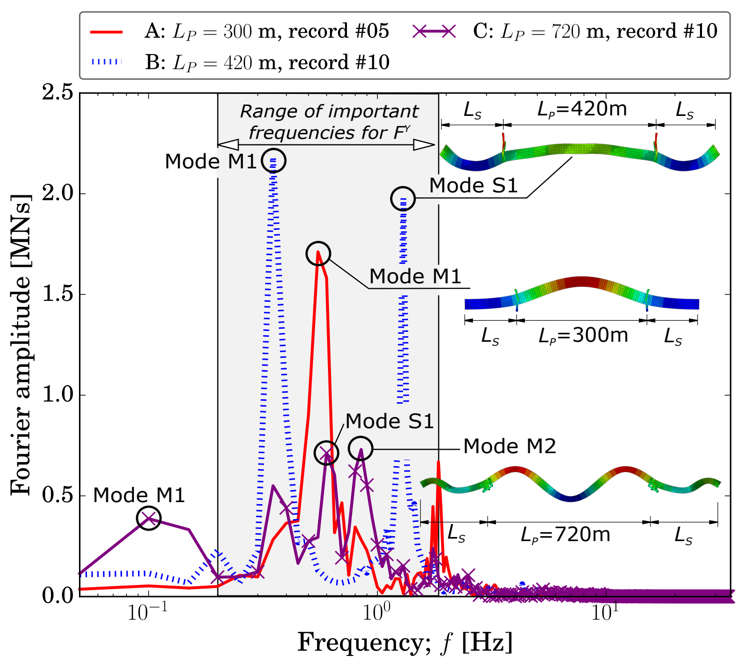

Figure 6: Frequency content of the deck-tower reaction time-history record. Labels A-C refer to Figure 5(b). The plan view of the most relevant vibration modes is included, removing the cable-system for illustration purposes.

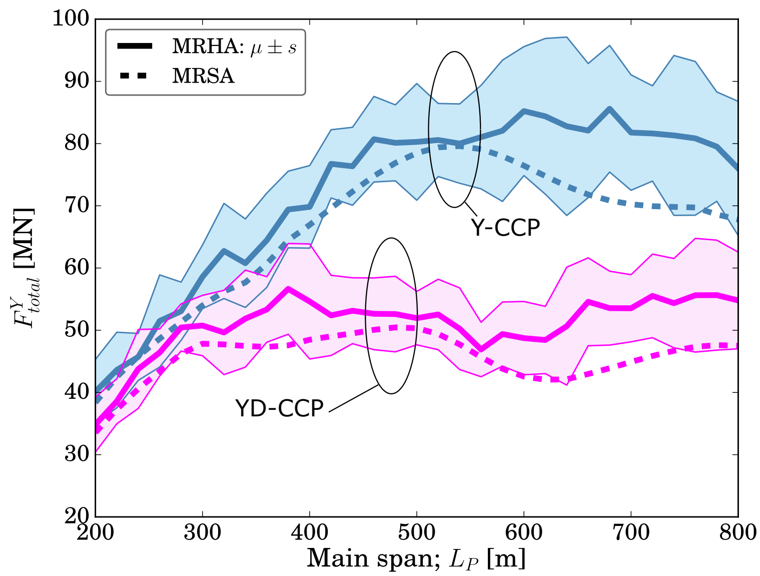

Figure 7: Peak deck-tower seismic reaction obtained with MRHA and MRSA (with only transverse modes included) in CCP models, soil TD, $H_i = H/2$, $B = 25$ m.

This is closely related to the interaction between the tower and the deck that was described in the modal analysis of Section 3. The transverse seismic response of cable-stayed bridges is dominated by vibration modes whose order increases with the span. Modes M1, S1 and M2 are dominant for moderate, medium and long spans, respectively. The total peak force exerted by the deck in the towers during the earthquake (F^Y_{total}) significantly increases when the contribution of one of these modes is maximum, which occurs for main spans close to the critical ones: $L_{PC,k}$, with k =M1, S1 and M2. In these cases F^Y_{total} is almost equal to the contribution of the corresponding governing mode, F^Y_k. This is observed in Figure 5(a), in which the maximum modal contribution is related to the corresponding modal shapes depicted in Figure 3. By increasing the main span length beyond the critical value $L_{PC,k}$, the weight of the k-th mode (F^Y_k) on the total response is strongly reduced due to the difference in the tower and the deck's flexibility associated with that mode. However, the next governing mode gains importance. In the border regions, in which two governing modes have similar participation, the seismic response is reduced.

The relative contribution of transverse modes different from M1, S1 and M2 has been also studied. Only symmetric modes have a significant influence on the transverse seismic response. This can be explained from the modal participation factor:

$$\Gamma_n = \frac{\boldsymbol{\phi}_n^T \mathbf{M} \boldsymbol{\iota}}{M_n} \tag{2}$$

where $M_n = \boldsymbol{\phi}_n^T \mathbf{M} \boldsymbol{\phi}_n$ is the modal mass; $\boldsymbol{\phi}$ is the transverse mode shape; $\mathbf{M}$ is the mass matrix of the structure; $\boldsymbol{\iota}$ is the influence matrix that links the degrees of freedom of the structure with the direction of the earthquake (in this case only transverse).

Due to the symmetry of the proposed structures, the shape of the transverse vibration modes ($\boldsymbol{\phi}$) is either symmetric or anti-symmetric with respect to the span centre (point CS in Figure 1). If the n-*th* mode is anti-symmetric, $\Gamma_n = 0$ because the modal displacement at the i-*th* node of the bridge is $\phi_{n,i}(x) = -\phi_{n,i}(-x)$ (x being the longitudinal distance from the span centre, positive to the right) and the diagonal terms of the mass matrix are always positive. Consequently, the contribution of anti-symmetric modes to the seismic response is null. This is in agreement with Zerva [31], who observed that synchronous ground motions with fully correlated waves (such as those considered in this study) only excite symmetric modes in 2- and 3-span beam bridges.

6. Influence of structural and ground motion features

6.1. Influence of the ground motion

The peak deck-tower reaction is strongly influenced by the shape of the design spectrum, defined in turn by the soil properties. F^Y_{total} is scaled up by a factor of 2 to 3 if the bridge is located on soft soil (TD), in comparison with the results for foundations on rock (TA). This increment in F^Y_{total} is directly proportional to the ratio between the TD and TA spectral accelerations in the range of low frequencies that dominates the response of cable-stayed bridges (from 0.2 to 1.8 Hz for the deck-tower reaction, according to Figure 6). However, it has been observed that the relative contribution of different modes is completely insensitive to the foundation soil. Only the seismic action defined from soft soil conditions (TD) is considered hereafter.

6.2. Influence of the tower shape

Figures 8 and 9 present the deck-tower reaction for different tower shapes in LCP and CCP arrangements, respectively. The results are completed with Figure 5(a) for the H-LCP bridge.

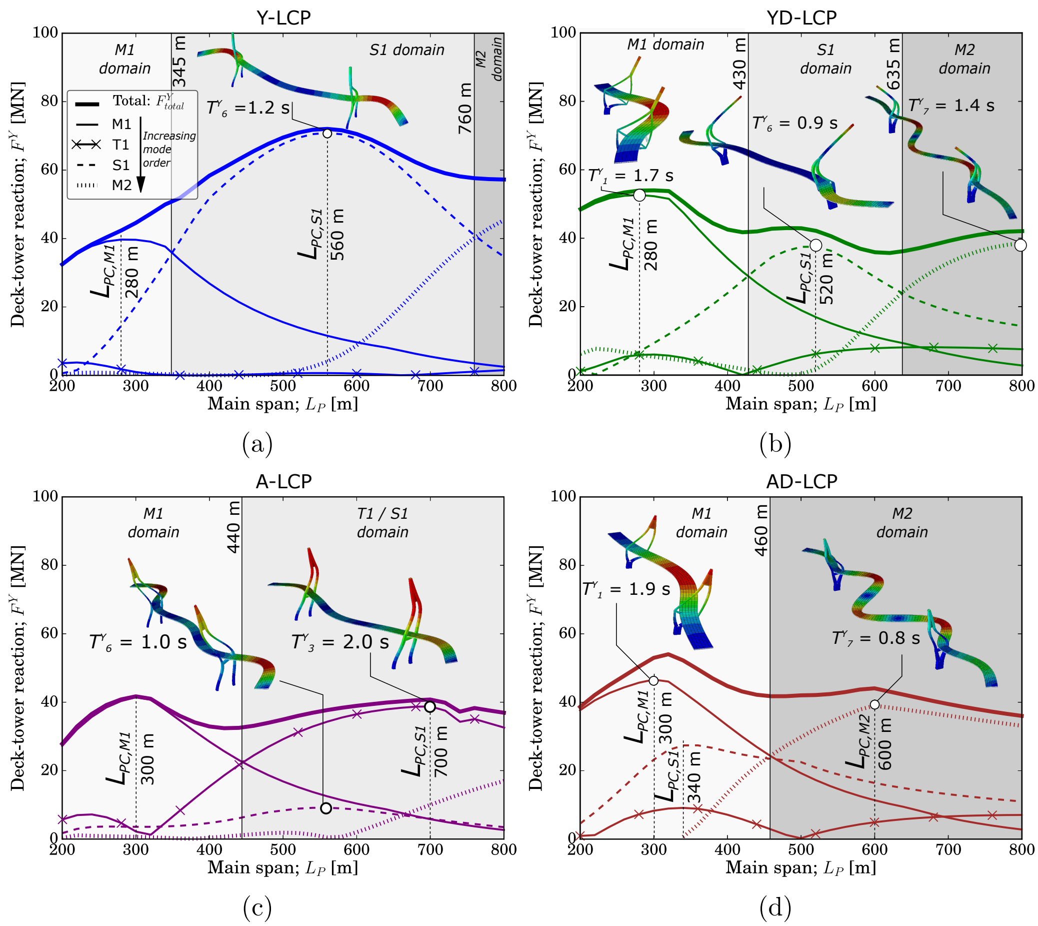

Figure 8: Modal contribution to the peak deck-tower seismic reaction in terms of the main span for LCP bridges: (a) Y-LCP, (b) YD-LCP, (c) A-LCP, (d) AD-LCP. $H_i = H/2$, $B = 25$ m, soil TD. The shape of relevant modes is included (cable-system removed for illustration purposes) along with their vibration periods T_n^Y.

The results show that it is possible to extend the range of spans in which the fundamental mode M1 is dominant (referred to as M1 domain), and to reduce in turn the domain of S1, by increasing the flexibility of the tower through the definition of its transverse geometry. This becomes apparent by

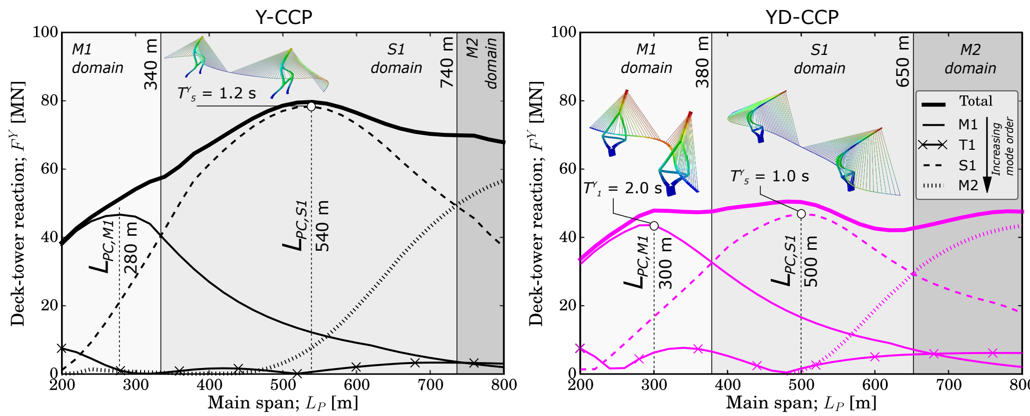

(a) (b)

Figure 9: Modal contribution to the peak deck-tower seismic reaction in terms of the main span for CCP bridges: (a) Y-CCP, (b) YD-CCP. $H_i = H/2$, $B = 25$ m, soil TD. The shape of relevant modes is included along with their vibration periods T_n^Y.

comparing the M1 domain in the stiff and flexible towers in Figures 8(a) and 8(b), respectively. Figure 8(b) shows that the M1 domain for the YD-LCP model includes main span lengths up to 430 m, whereas this limit is reduced to 345 m in the homologue towers without lower diamond (Y-LCP, Figure 8(a)). On the contrary, the width of the S1 domain in bridges with stiff towers almost doubles the one observed with flexible towers (from 240 to 410 m in the figures included, on average). But more importantly, the maximum contribution of S1 to the deck-tower reaction significantly increases in bridges with 'Y'-shaped towers. This is remarkable in the structures with main spans ranging between 500 and 600 m: F^Y_{total} is almost two times larger in Y-LCP and Y-CCP models than in bridges with other towers, as it is observed in Figures 8(a) and 9(a). In light of these results, inverted 'Y'-shaped towers would not be recommended for cable-stayed bridges with medium-to-long spans located in seismic regions.

A-LCP bridges present reduced deck-tower reactions in comparison with the homologue Y-LCP models. This is clear when comparing Figures 8(a) and 8(c) throughout the complete span range, but particularly beyond the M1 domain, reaching a maximum 60% reduction in F^Y_{total} for $L_P = 500$ m. Figure 8(c) shows that the contribution of several modes in A-LCP bridges differs from the rest of the cases. This is because of the participation of vibration modes that mainly involve the transverse response of the towers (referred to as T1). Mode T1 has only a minor contribution to the total seismic response in bridges with different tower shapes: it is typically around 5% of the total deck-tower reaction in bridges with inverted ‘Y’-shaped towers, and 20% in other models. However, in A-LCP bridges with medium-to-long spans (beyond 440 m) this mode is dominant as it is coupled with the transverse flexure of the side and main spans, being referred to as T1/S1 mode in Figure 8(c). Mode S1 can also be identified in A-LCP models, but its participation is reduced and it is rarely dominant for the span range studied. This is also observed for ‘A’-shaped towers with lower diamond (see Figure 8(d)). It is attributed to the transverse connection between the legs at the anchorage area of ‘A’-shaped towers, where a significant mass is concentrated and a characteristic transverse rigid body motion is observed in the seismic response (see Figure 2). This favours the transverse displacement at the level of the deck in the first-order tower mode and the deck-tower interaction (T1/S1 mode).

6.3. Influence of the cable-system arrangement

The deck-tower reaction is approximately 15% larger in bridges with one Central Cable Plane (CCP, Figures 9(a) and 9(b)), in comparison with the homologue models with lateral cable arrangement (LCP, Figures 8(a) and 8(b)). This is partly because the closed-section deck in CCP models is heavier than the open-section girder of LCP structures (from 10 to 20% in 200 and 800 m span bridges, respectively). In order to isolate the dynamic effect of the cable-system, the deck-tower reaction in Figure 10(a) is normalised with respect to the tributary static weight of the deck that contributes to the tower reaction in the transverse direction:

$$W^{Y}_{trib,S} = m_d \left(\frac{L_P + L_S}{2} \right) g \tag{3}$$

where m_d is the mass per unit length of the deck (including the structural and non-structural mass); $L^{Y}_{trib,S} = (L_S + L_P)/2$ is the tributary static length of the deck that corresponds to the transverse support at the towers; $g = 9.81$ m/s^2 is the gravitational acceleration.

From the normalised results in Figure 10(a), the differences in the seismic response due to the cable-arrangement are only appreciable for short spans, below 350 m. In this span range the vibration mode M1 is dominant and it increases the deck-tower reaction in CCP models up to 9%, with respect to LCP bridges. This can be explained by the different configuration of the

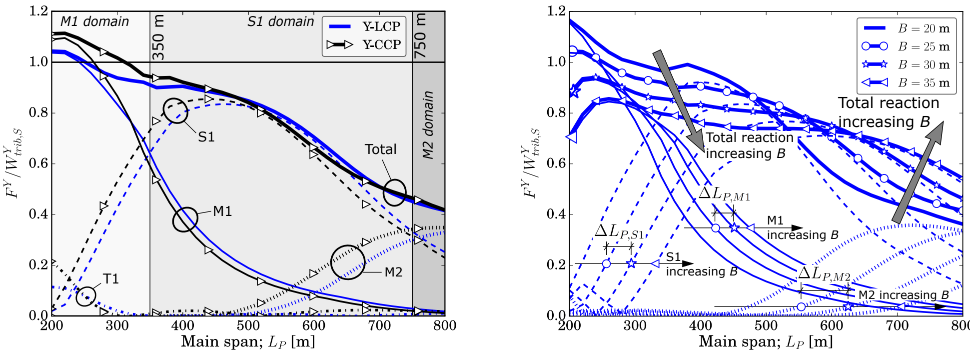

(a) (b)

Figure 10: Normalised peak deck-tower seismic reaction in inverted 'Y'-shaped tower bridges: (a) influence of the cable arrangement ($B = 25$ m), (b) influence of the deck width (B) in the Y-LCP model. $H_i = H/2$.

cable anchorages along the deck in CCP and LCP models. If the cables are perpendicular to the deck (as it is the case in CCP models) the transverse seismic loads coming from the girder can only be transmitted to the tower through the deck-tower connection (neglecting the small nonlinear geometric contribution of the cables to the transverse stiffness of the bridge). However, bridges with two cable planes anchored at the girder edges (LCP) provide an additional path to transmit the lateral deck loads through the inclined cable-system to the towers and their foundations. The normalised deck-tower reaction is almost independent of the cable-arrangement when the dominant mode is S1 or M2, i.e. for medium-to-large main spans (above 400 m). This can be also explained in the context of the transverse cable inclination: the cables are almost vertical in LCP arrangements for large main spans due to the small B/H ratio, and therefore their configuration is similar to CCP models. Consequently, by increasing the width of the deck (B) the effect of the cable arrangement is more significant and affects bridges with longer span lengths: in the 600 m span bridges with $B = 35$ m the normalised deck-tower reaction is 9% larger in Y-CCP than Y-LCP.

Figure 10(a) also shows the dynamic amplification of the deck-tower reaction with respect to the corresponding static value for short-span bridges (below 300 m span): i.e. $F^Y/W^Y_{trib,S} > 1$. This ratio decreases monotonically by increasing the separation distance between towers. Although it is observed that high-order modes have a dominant role in the seismic response of long-span bridges, the overall effect is that in these structures the deck reaction is significantly smaller than the tributary static weight of the deck in the towers in the transverse direction, down to 40% for $L_P = 800$ m.

6.4. Influence of the deck width and height: B, H_i

The width of the deck (B) and its distance from the foundation of the towers (H_i) are typically constrained by the project requirements and, therefore, they can hardly be modified by designers. However, it is important to explore their influence on the seismic response.

Figure 10(b) shows the normalised deck-tower reaction in the Y-LCP model for different values of B. Any increment of B shifts in a constant value (ΔL_P) the modal contribution curve towards larger main spans (L_P), increasing the critical span lengths accordingly ($L_{PC,k}$, with k =M1, S1 and M2). This is due to the strong (cubic) increment of the transverse flexural stiffness of the deck (EI^Y) with its width, and it is more pronounced the higher the mode order: $\Delta L_{P,M1} < \Delta L_{P,S1} < \Delta L_{P,M2}$, as it is observed in Figure 10(b). By increasing B, the normalised modal contribution at the critical main span usually decreases because the maximum deck-tower interaction occurs for larger values of L_P. The global effect of the variation of B in the deck-tower reaction depends on the main span due to the 'bell' shape of the modal contribution curves. If $L_P < L_{PC,k}$ the k-th modal contribution decreases by increasing B, and vice-versa for $L_P > L_{PC,k}$. After the combination of different vibration modes, increasing B typically reduces the normalised deck-tower reaction in the short-span range. Bridges with inverted 'Y'-shaped towers are very sensitive to the contribution of mode S1 and, consequently, to any variation of B. These bridges present two distinct zones of the span range in which the influence of B is opposite, as it is shown in Figure 10(b): a reduction of F^Y down to 60% is observed in the 200 m span Y-LCP bridge (200 m $< L_{PC,M1}$) by increasing B from 20 to 35 m, whereas the same variation in B results in a 42% increment of F^Y in the 800 m bridge (800 m $> L_{PC,k}$, with k =M1, S1 and M2). The other bridge typologies are less sensitive to changes in B.

It is observed that larger values of H_i generally lead to smaller deck-tower reactions in the entire span range. However, in AD-LCP bridges F^Y is almost doubled by increasing 66% the tower height. This is attributed to the larger flexibility of the vertical pier in the lower diamond configuration.

7. Critical main span lengths and tower frequencies

From the previous discussion it is clear that there is a relationship between the seismic response of the bridge and the vibration modes of the towers and the deck. Figures 11 - 13 present the contribution of different modes to the deck-tower reaction in terms of the ratio between the nth-order vibration frequencies of the deck ($\omega_{d,n}$) and the tower ($\omega_{t,n}$), obtained separately. These figures include the results in all the proposed models and distinguish the tower-shape, but not L_P, B and H_i. The results demonstrate that there is a direct relationship between the deck-tower reaction and their isolated vibration frequencies. This is satisfied in all the models and allows for design recommendations that are applicable to a wide range of cable-stayed bridges. $\omega_{d,n}$ can be estimated from Eq. (1), considering that the transverse vibration of the deck is equivalent to that of a single-span beam with a certain length and boundary conditions. The specific values for this expression are discussed below for different modes. FE models of the tower have been employed to obtain $\omega_{t,n}$.

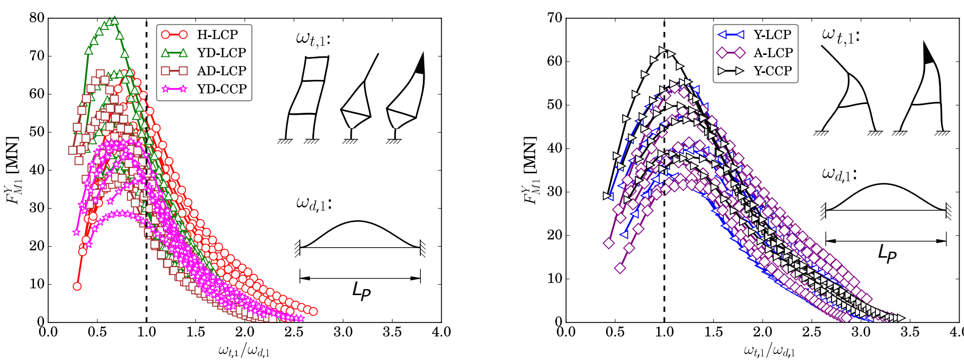

(a) (b)

Figure 11: Contribution of mode M1 to the peak deck-tower seismic reaction in terms of the ratio of the tower and deck frequencies: (a) flexible towers, (b) stiff towers. All models. Soil TD.

Figure 11 presents the contribution of M1 to the deck-tower reaction (F^Y_{M1}). When the fundamental frequency of the deck is close to that in the tower, i.e. when $\omega_{t,1}/\omega_{d,1} = \beta$ (typically $0.8 < \beta < 1.2$), the seismic response is maximised. Analogously, the coupling between the deck and the tower frequencies is responsible for the increment in the contribution of mode S1,

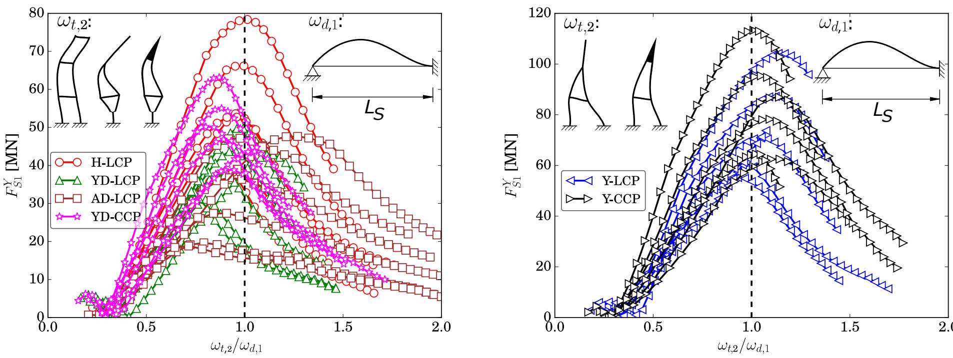

(a) (b)

Figure 12: Contribution of mode S1 to the peak deck-tower seismic reaction in terms of the ratio of the tower and deck frequencies: (a) flexible towers, (b) stiff towers. All models. Soil TD.

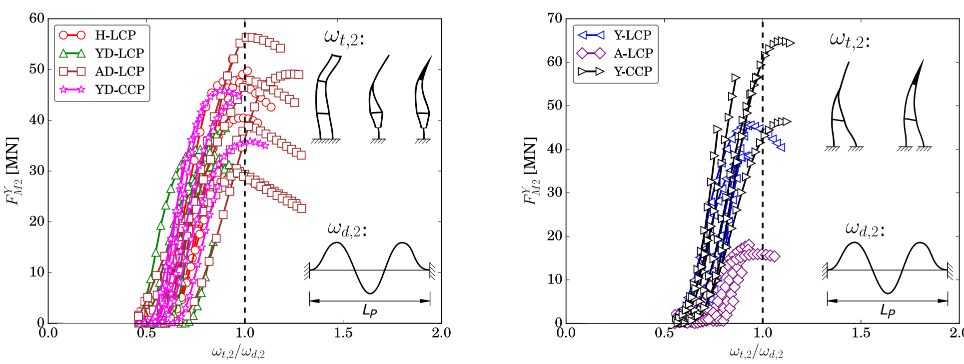

(a) (b)

Figure 13: Contribution of mode M2 to the peak deck-tower seismic reaction in terms of the ratio of the tower and deck frequencies: (a) flexible towers, (b) stiff towers. All models. Soil TD.

as shown in Figure 12. In this case, if the first-order vibration of the lateral spans is close to the second-order vibration of the towers, i.e. $\omega_{t,2}/\omega_{d,1} = \beta \approx 1$, then F^Y_{S1} is maximised. Figure 13 shows that the contribution of mode M2 reaches its maximum expression when the second-order symmetric flexure of the main span is coupled with the second order vibration of the towers, i.e. $\omega_{t,2}/\omega_{d,2} = \beta \approx 1$. This proves that the interaction between the deck and the towers is maximised, and may lead to large seismic forces, if the vibration frequencies of both members are similar. This coupling occurs if the main span of the bridge coincides with the critical lengths: $L_{PC,k}$, where $k =$M1, S1 and M2. Figures 11 - 13 also verify, now for all the studied bridges, that if the main span length is well above the k-th critical span ($L_P > L_{PC,k}$) the deck is too flexible to interact with the towers in that vibration mode, because $\omega_t/\omega_d > 1$. And vice-versa for $L_P < L_{PC,k}$, as $\omega_t/\omega_d < 1$.

The frequency ratio for which the modal contribution is maximum, $\omega_{t,n}/\omega_{d,n} = \beta$, is biased with respect to the point in which the isolated tower and deck frequencies coincide exactly (i.e. $\beta \neq 1$), especially in mode M1. This is due to the modification of the vibration modes of the tower and the deck when both elements are connected. Eq. (1) assumes that the supports of the beam model, which represent the effect of the tower, are fixed in the transverse direction. However, when the modal interaction between the deck and the towers is maximum, the latter move transversely (especially for mode M1, see cell A1 in Figure 3), which is not captured by Eq. (1). This effect is taken into account by the parameter β in Table 1. The proposed values of β distinguish the shape of the towers and are obtained from the arithmetic average of the frequency ratios (ω_t/ω_d) in which the modal contribution is maximum for different values of B and H_i (although these parameters hardly affect the frequency ratios). It is observed that β is influenced by the tower geometry, resulting $\beta < 1$ for flexible towers ('H'-shaped and lower diamond towers) and $\beta > 1$ for stiff towers (with inverted 'Y'- and 'A'-shaped geometries).

The critical main span can be estimated from these results and Eq. (1), by imposing that $\omega_t/\omega_d = \beta$:

$$L_{PC,k} \approx C\sqrt{A}\sqrt[4]{\frac{EI_d\beta^2}{m_d\omega_{t,n}^2}} \tag{4}$$

where $k =$M1, S1 and M2 is the vibration mode in which the seismic response is maximised for the corresponding critical main span; C is a constant to take into account the length of the deck that is involved in the vibration mode, i.e. the main span (L_P) or the side span (L_S). The values of A, C, β and n are included in Table 1 for different modes and tower shapes. A depends on the rotation of the deck at the ends of the beam model, which is included in Figures 11 - 13. Considering mode M1, the rotation of the deck about the vertical axis (θ_Z) is constrained at the tower level due to the negligible displacement in the side spans. Consequently, ω_d is estimated in mode M1 by considering a beam of length L_P that is completely fixed at the ends ('fixed-fixed' conditions). The same beam length and boundaries are employed for the critical span in mode M2, but adopting the second-order symmetric mode ($n = 2$). The situation is different in mode S1 as the side span behaves like a beam that is pinned at the abutment (where the support bearings allow for θ_Z rotations, see abutment A1 in Figure 1) and fixed at the level of the tower, due to the constraint of the main span.

		'Flexible' towers				'Stiff' towers		
Mode		H-LCP	YD-LCP	AD-LCP	YD-CCP	Y-LCP	A-LCP	Y-CCP
k =M1	A	22.4	22.4	22.4	22.4	22.4	22.4	22.4
	C	1.00	1.00	1.00	1.00	1.00	1.00	1.00
	β	0.78	0.68	0.63	0.79	1.21	1.17	1.10
	n	1	1	1	1	1	1	1
k =S1	A	15.4	15.4	15.4	15.4	15.4	-	15.4
	C	L_P/L_S	L_P/L_S	L_P/L_S	L_P/L_S	L_P/L_S	-	L_P/L_S
	β	0.96	0.92	*	0.91	1.04	-	1.07
	n	2	2	2	2	2	-	2
k =M2	A	120.9	120.9	120.9	120.9	120.9	120.9	120.9
	C	1.00	1.00	1.00	1.00	1.00	1.00	1.00
	β^{**}	0.94	0.82	1.00	0.96	1.00	0.97	1.10
	n	2	2	2	2	2	2	2

Table 1: Parameters involved in Eqs. (4) and (5) for different bridge models. (*) the maximum contribution of S1 is observed in a band of frequency ratios $\beta = [0.85, 1.12]$ in AD-LCP. (**) β is obtained from a reduced number of cases in M2. The parameters are not provided for the mode S1 in the bridge A-LCP since it is not governing (see Figure 8(c)).

It is important to note that the critical spans in which the modal contributions are amplified in Eq. (4) are more sensitive to the tower frequency (affected in turn by the tower geometry) than to the deck stiffness or mass.

This is very advantageous from the design point of view since the deck properties are constrained by the project requirements and are difficult to change. However, the tower shape can be designed to avoid potential couplings with the deck at regions where $\omega_t/\omega_d = \beta$. Therefore, the tower vibration frequency should be away from the following three critical frequencies:

$$\omega_{tc,n}^{k} = A\beta C^2 \sqrt{\frac{EI_d}{m_d L_P^4}} \tag{5}$$

where k =M1, S1 and M2. The rest of the parameters are included in Table 1.

Short-span bridges are more likely to be affected by the critical frequency corresponding to mode M1 ($\omega_{tc,1}^{M1}$). In the range of medium-to-long span bridges (400 m $< L_P <$ 700 m), the inverted 'Y'-shaped towers can have frequencies that are potentially close to $\omega_{tc,2}^{S1}$, as it has been observed in this work. In these cases, it would be recommended to connect the tower legs below the deck in a lower diamond configuration, which reduces the second-order frequency of the tower below $\omega_{tc,2}^{S1}$.

Note that expressions (4) and (5) are valid only for conventional cable-stayed bridges with the arrangement described in Figure 1.

8. Conclusions

This work is focused on the transverse seismic response of more than 1050 cable-stayed bridges with main span lengths ranging from 200 to 800 m. The study explores the contribution of different vibration modes and the influence of structural and ground motion features on the peak transverse deck-tower reaction. The Modal Response Spectrum Analysis (MRSA) is selected after a complete validation procedure, considering the modal time-history analysis as the reference. The results in time- and frequency-domain show that the MRSA, when applied to finite element models that only capture the transverse response, represents accurately the contribution of different vibration modes to the deck-tower reaction. The main outcomes of this study are summarised as follows:

- The contribution of transverse vibration modes to the seismic response is strongly influenced by the main span length. It is maximised for certain (critical) main spans in which the modal shape involves the deformation of both the towers and the deck. The modal contribution is reduced for main spans above the critical value due to the large flexibility of the deck with respect to the towers. As a result, the dynamic response of the deck interacts with the towers in vibration modes of increasingly higher order. These modes are dominant for long-span bridges and need to be accounted for in the design and analysis.

- Three different transverse vibration modes that govern the seismic response of cable-stayed bridges in different span ranges have been identified. Short-to-medium span bridges (below 400 m) are dominated by a vibration mode that involves the first-order transverse flexure of the deck in the main span and the towers (mode M1). Medium-to-long span bridges (between 400 and 600 m) are usually governed by the interaction between the side spans and the towers in the transverse direction (mode S1). Finally, long-span bridges (above 600 m) are strongly influenced by a transverse vibration mode that involves the second-order flexural response of the tower and the deck in the main span (mode M2). Only the symmetric modes have a significant contribution to the seismic response of symmetric cable-stayed bridge under synchronous ground motions.

- The contribution of the governing vibration modes has been represented in terms of the ratio between the deck and the tower vibration frequencies for all the models, being always maximum when this ratio falls between 0.8 and 1.2. Analytical expressions are proposed to calculate the critical span lengths and the tower frequencies for which the transverse seismic response is maximised. These are more influenced by the tower shape than by the deck properties, which opens the door for conceptual designs that optimise the tower geometry in order to avoid potentially catastrophic deck-tower interactions during the earthquake.

- The inclination of the lateral legs of the tower above and below the deck significantly affects the transverse seismic response of the bridge. The more inclined the legs above the deck the larger the transverse stiffness of the tower, which can lead to significant increments of the seismic response in bridges with main span lengths between 500 and 600 m. By connecting the legs below the deck in a lower diamond configuration, the transverse stiffness of the towers can be reduced, which also decreases the seismic demand in medium-span structures.

- The inclination of the cable planes is also relevant for the transverse seismic response of the bridge. The deck-tower reaction is generally reduced (down to 9%) in bridges below 400 m span with two lateral cable planes, in comparison with the central cable plane configuration. This effect is stronger the shorter the span and the wider the deck, especially in bridges with inverted 'Y'-shaped towers.
- The seismic deck-tower reaction in long-span bridges is a small fraction of the corresponding (static) weight of the deck. This suggests that the effect of the deck on the towers is less problematic in large bridges than in small bridges (below 300 m span), where significant dynamic amplifications have been observed.

References

[1] K. Kawashima, S. Unjoh, Seismic behaviour of cable-stayed bridges, in: Cable-stayed Bridges; Recent Developments and their Future, Elsevier science Ltd., Yokohama (Japan), 1991, pp. 193–212.

[2] A. Abdel-Ghaffar, Cable - stayed bridges under seismic action, in: Cable - stayed Bridges; Recent Developments and their Future, Elsevier Science Ltd., Yokohama (Japan), 1991, pp. 171–192.

[3] A. Camara, M. Astiz, A. Ye, Fundamental mode estimation for modern cable-stayed bridges considering the tower flexibility, Journal of Bridge Engineering 19 (2014) 04014015–1/12.

[4] E. Caetano, A. Cunha, C. Taylor, Investigation of dynamic cable-deck interaction in a physical model of a cable-stayed bridge. part ii: Seismic response, Earthquake engineering and structural dynamics 29 (2000) 481–498.

[5] W. He, A. Agrawal, K. Mahmoud, Control of seismically excited cable-stayed bridge using resetting semiactive stiffness dampers, Journal of Bridge Engineering (2001) 376–384.

[6] N. Gimsing, Cable supported bridges: Concept and design, John Wiley and Sons, 1998, second edition.

[7] R. Walther, B. Houriet, W. Isler, P. Moia, Cable-stayed bridges, Thelford, 1988.

[8] A. Ye, S. Hu, L. Fan, Seismic conceptual design of a three-tower cable-stayed bridge, in: IABSE symposium 2002; Towards a Better Built Environment Innovation, Sustainability, Information and Technology, Melbourne (Australia), 2002.

[9] H. Ali, A. Abdel-Ghaffar, Modelling the non linear seismic behaviour of cable - stayed bridges with passive control bearings, Computers and Structures 54(3) (1995) 461–492.

[10] A. Nazmy, A. Abdel-Ghaffar, Effects of ground motion spatial variability on the response of cable-stayed bridges, Earthquake engineering and structural dynamics 21 (1992) 1–20.

[11] D. Siringoringo, Y. Fujino, Observed dynamic performance of the yokohama-bay bridge from system identification using seismic records, Journal of Structural Control and Health Monitoring 13(1) (2005) 226–244.

[12] W. Liu, X. Xu, R. Wang, Z. Wang, X. Wu, Vibration reduction design of the hangzhou bay cable-stayed bridges, Structural Engineering and Mechanics 24(3) (2006) 339–354.

[13] A. Camara, Seismic behaviour of cable-stayed bridges: design, analysis and seismic devices, Ph.D. thesis, ETSI Caminos Canales y Puertos, Universidad Politécnica de Madrid (UPM), Madrid (Spain) (2011).

[14] A. Camara, M. Astiz, Analysis and control of cable-stayed bridges subject to seismic action, Structural Engineering International 24 (1) (2014) 27–36.

[15] A. Camara, M. Astiz, Typological study of the elastic seismic behaviour of cable-stayed bridges, in: Proceedings of the Eighth European Conference on Structural Dynamics (2011), Leuven (Belgium), 2011.

[16] K. Chang, Y. Mo, C. Chen, L. Lai, C. Chou, Lessons learned from the damaged chi-lu cable-stayed bridge, Journal of Structural Engineering 9 (4) (2004) 343–352.

[17] T. Wyatt, The dynamic behaviour of cable-stayed bridges: fundamentals and parametric studies, in: Cable - stayed Bridges; Recent Developments and their Future, Elsevier Science Ltd., Yokohama (Japan), 1991, pp. 151–170.

[18] A. Camara, M. Astiz, Pushover analysis for the seismic response prediction of cable-stayed bridges under multi-directional excitation, Engineering Structures 41 (2012) 444 – 455.

[19] D. Chen, F. Au, L. Tham, P. Lee, Determination of initial cable-forces in prestressed concrete cable-stayed bridges for given design deck profiles using the force equilibrium method, Computers and structures 74 (2000) 1 – 9.

[20] P. Lonetti, A. Pascuzzo, Optimum design analysis of hybrid cable-stayed suspension bridges, Advances in Engineering Software 73 (2014) 53 – 66.

[21] F. Ferreira, L. Simoes, Optimum design of a controlled cable stayed bridge subject to earthquakes, Struct Multidisc Optim 44 (2011) 517 – 528.

[22] G. Calvi, T. Sullivan, A. Villani, Conceptual seismic design of cable-stayed bridges, Journal of Earthquake Engineering 18 (8) (2010) 1139 – 1171.

[23] T. Hayashikawa, Y. Matsui, T. Kaneko, Nonlinear dynamic behaviour and seismic isolation of steel towers of cable - stayed bridges under great earthquake ground motion, in: 12th World Conference on Earthquake Engineering, Auckland (New Zealand), 2000, paper No. 0469.

[24] Abaqus, Finite element analysis program; version 6.13, Providence USA (2015).

[25] Eurocode 1 Part 2: Traffic loads on bridges, eN 1991-2:2003 (2003).

[26] Eurocode 4: Design of composite steel and concrete structures - Part 2: General rules and rules for bridges, eN 1994-2:2005 (2005).

[27] Y. Ni, J. Wang, J. Ko, Modal interaction in cable-stayed ting kau bridge, available at:
http://www.cse.polyu.edu.hk/ dynamics/assets/pdf/p-asd-wjy2.pdf (accessed 06/04/2015) (2000).

[28] M. Astiz, Specific wind problems affecting composite bridges, in: III Meetings on composite bridges, Madrid (Spain), 2001.

[29] EC8, Eurocode 8: Design of structures for earthquake resistance. part 1: General rules, seismic actions and rules for buildings, eN 1998-1:2004 (2004).

[30] A. Camara, , M. Astiz, Applicability of the strategies for the elastic seismic analysis of cable-stayed bridges, Revista internacional de metodos numericos para calculo y diseno en ingenieria (In Spanish) 30 (1) (2014) 43 – 50.

[31] A. Zerva, Response of multi-span beams to spatially incoherent seismic ground motions, Earthquake Engineering and Structural Dynamics 19 (1990) 819–832.